

Project Title:

**Numerical study on new functionality of spin-heat cross effect**

Name: Qinfang Zhang

Laboratory: Computational Condensed Matter Physics Laboratory,  
RIKEN Advanced Science Institute, RIKEN Wako Institute**I. Introduction**

Transition-metal oxides in perovskite-based structures exhibit a wide variety of phases with different electronic, magnetic, and orbital structures, and show rich functionalities such as high- $T_c$  superconductivity, colossal magnetoresistance, and multiferroics. A recent advance in epitaxial growth techniques has made it even possible to fabricate transition-metal oxide heterostructures with sharp and smooth interfaces controlled at the atomic scale. In these heterostructures, many unique properties, not found in the corresponding alloy compounds made of the same composite elements, have been observed, which include, e.g., two dimensional electron gas with high mobility at the heterostructure interfaces, indicating the promising potential of oxide heterostructures for future technological applications.

In the case of manganites,  $\text{LaMnO}_3$  is an A-type antiferromagnetic insulator and  $\text{SrMnO}_3$  is a G-type antiferromagnetic insulator. On one hand, the randomly cation-doped alloy  $\text{La}_{1-x}\text{Sr}_x\text{MnO}_3$  exhibits a rich magnetic phase diagram, depending on the doping concentration  $x$ . On the other hand, La/Sr cation-ordered analogs forming superlattices behave quite differently from their alloy compounds. For example,  $\text{La}_{2/3}\text{Sr}_{1/3}\text{MnO}_3$  alloy has a mixed valence of  $\text{Mn}^{3+}/\text{Mn}^{4+}$ , and the ground state is ferromagnetic half metallic due to the double-exchange mechanism. To the contrary, it is found experimentally that cation-ordered  $(\text{LaMnO}_3)_{2n}/(\text{SrMnO}_3)_n$  (001) superlattices are insulating when  $n$  is larger than 3. This change of behavior is easily understood because the number  $n$  of  $\text{SrMnO}_3$  layers control the quantum confinement potential: when  $n$  is small, the

confinement potential is small and the  $eg$  electrons are distributed uniformly, thus expecting the phases similar to the alloy  $\text{La}_{1-x}\text{Sr}_x\text{MnO}_3$ . When  $n$  is large, the confinement potential becomes large enough to trap the  $eg$  electrons in  $\text{LaMnO}_3$  layers, and thus the bulk properties of  $\text{LaMnO}_3$  and  $\text{SrMnO}_3$  would be observed. Several theoretical studies for  $(\text{LaMnO}_3)_{2n}/(\text{SrMnO}_3)_n$  superlattices have been reported to understand their electronic and magnetic properties. More recently, Bhattacharya *et al.* have experimentally studied the transport and the magnetic properties of similar superlattices  $(\text{LaMnO}_3)_n/(\text{SrMnO}_3)_{2n}$  grown on  $\text{SrTiO}_3$  (001) substrate. They have found that the ground state of these superlattices with  $n = 1, 2$  are A-type antiferromagnetic metals with Néel temperature ( $T_N$ ) which is higher than that observed in any alloy  $\text{La}_{1-x}\text{Sr}_x\text{MnO}_3$  compound. Although the similar physical principles found in  $(\text{LaMnO}_3)_{2n}/(\text{SrMnO}_3)_n$  superlattices are certainly expected to apply here, the systematic theoretical investigations are required to understand the main ingredients which determine the electronic as well as the magnetic properties of  $(\text{LaMnO}_3)_n/(\text{SrMnO}_3)_{2n}$  superlattices. Here, in this paper, performing first-principles calculations based on the density functional theory, we study the electronic and the magnetic structures of  $(\text{LaMnO}_3)_n/(\text{SrMnO}_3)_{2n}$  (001) superlattices with  $n = 1, 2$ . We show that the magnetic properties are governed not only by the quantum confinement potential caused by periodic alignment of cation ions  $\text{La}^{3+}/\text{Sr}^{2+}$ , but also by the strain induced by substrates on which the superlattices are grown. Namely, for the case of tensile strain induced by  $\text{SrTiO}_3$  (STO) (001) substrate, our calculations show that the

ground state of these superlattices are A-type antiferromagnetic and  $d_{x^2-y^2}$  orbital ordered with higher  $T_N$  for  $n = 1$  than for  $n = 2$ . This is indeed in excellent agreement with recent experimental observations. Instead, for the case of compressive strain induced by LaAlO<sub>3</sub> (LAO) (001) substrate, we predict C-type antiferromagnetic and  $d_{3z^2-r^2}$  orbital orders with higher  $T_N$  for  $n = 1$  than for  $n = 2$ .

## II. COMPUTATIONAL METHODS

We perform the first-principles electronic-structure calculations based on the projected augmented wave pseudopotentials using the Vienna *ab initio* simulation package (VASP). The valence states include  $3d^5 4s^1$  and  $2s^2 2p$  for Mn and O, respectively. The electron interactions are described using the generalized gradient approximation (GGA) and the rotationally invariant GGA+ $U$  method with the effective  $U_{\text{eff}}$ , i.e.,  $U - J$ , from 1 to 5 eV for  $d$  electron states. Compared to the GGA, the GGA+ $U$  approach gives an improved description of  $d$  electron localization. The atomic positions of superlattices are fully optimized iteratively until the Hellman-Feynman forces are 0.01 eV/Å or less. The plane-wave cutoff is set to be 500 eV and a  $12 \times 12 \times 12$  Monkhorst-Pack  $k$ -point grid is used in combination with the tetrahedron method.

The supercells considered here consist of six MnO<sub>2</sub> layers, two LaO layers, and four SrO layers for both  $n = 1$  and 2. We consider 12 and 10 different magnetic moment alignments to search for the ground-state magnetic structures for LaMnO<sub>3</sub>(SrMnO<sub>3</sub>)<sub>2</sub> and (LaMnO<sub>3</sub>)<sub>2</sub>(SrMnO<sub>3</sub>)<sub>4</sub> superlattices, as shown in Figs. 1 and 2, respectively. These magnetic structures include not only simple ferromagnetic, A-type, C-type, and G-type antiferromagnetic structures, but also magnetic structures with mixed combinations of these simple magnetic structures. The epitaxial constraint on these superlattices, which is grown on substrates, is to fix the in-plane lattice constants. Thus, to simulate the strain effect, we fix the in-plane lattice

constants ( $a$ ) of the superlattices to those of substrates, i.e.,  $a = 3.905$  Å for SrTiO<sub>3</sub> substrate and  $a = 3.81$  Å for LaAlO<sub>3</sub> substrate, and the lattice constant ( $c$ ) perpendicular to MnO<sub>2</sub> layers is fully relaxed. Atomic positions are also fully optimized.

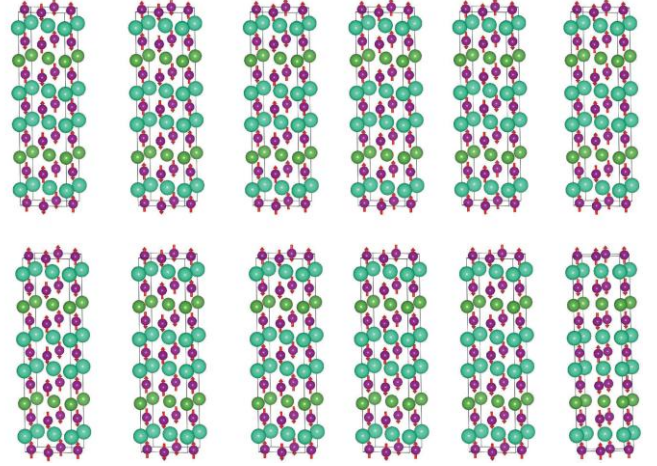


Fig.1 12 different magnetic structures considered for LaMnO<sub>3</sub>/(SrMnO<sub>3</sub>)<sub>2</sub> superlattices: G-AFM (a), C-AFM (b), M1-AFM (c), FM (d), M2-AFM (e), D-AFM (f), A-AFM (g), M3-AFM (h), M4-AFM (i), M5-AFM (j) M6-AFM (k), and D1-AFM. Mn spins are indicated by arrows. Aqua, lime and violet spheres stand for Sr, La, and Mn atoms, respectively. O atoms are omitted for clarity.

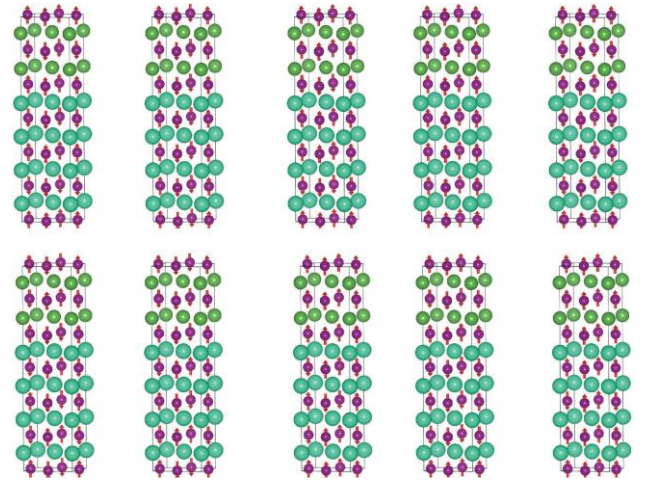


Fig.2. 10 different magnetic structures considered for (LaMnO<sub>3</sub>)<sub>2</sub>/(SrMnO<sub>3</sub>)<sub>4</sub> superlattices: A-AFM (a), C-AFM (b), D-AFM (c), FM (d), M2-AFM (e), G-AFM (f), M1-AFM (g), M3-AFM (i), and M5-AFM (j). Mn spins are indicated by arrows. Aqua, lime, and violet spheres stand for Sr, La, and Mn atoms, respectively. O atoms are omitted for clarity.

### III. RESULTS

#### A. $(\text{LaMnO}_3)_n(\text{SrMnO}_3)_{2n}$ on $\text{SrTiO}_3$

Let us first examine  $(\text{LaMnO}_3)_n(\text{SrMnO}_3)_{2n}$  (001) superlattices on  $\text{SrTiO}_3$  (001) substrate. Our systematic GGA calculations reveal that the ground states of these superlattices with  $n = 1$  and  $2$  are both A-type antiferromagnetic metals. A schematic spin alignment of A-type antiferromagnetic order is shown in Figs. 1(g) and 2(a). Indeed the projected spin-density distribution, calculated by integrating spin density of occupied states from Fermi level down to  $-0.5$  eV, clearly indicates the A-type antiferromagnetic spin order. Our GGA+U calculations also find that these A-type antiferromagnetic states are robust against electron correlations, and they are indeed stable up to  $U_{\text{eff}} = 2$  eV for  $n = 1$  and  $U_{\text{eff}} = 1.3$  eV for  $n = 2$  (see Fig. 3).

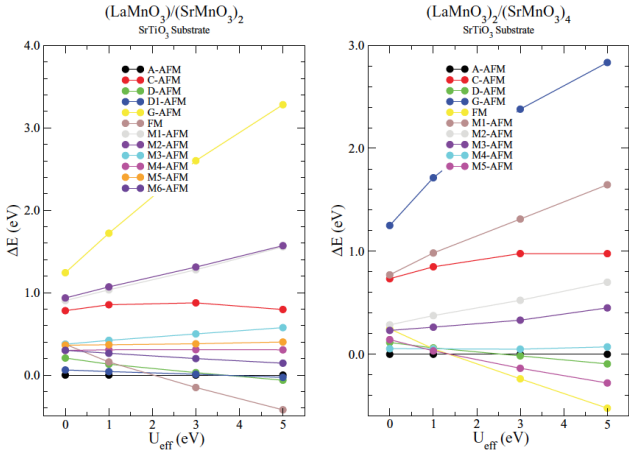


Fig.3  $U_{\text{eff}}$  dependence of the relative energies (calculated using GGA+U) for various magnetic structures compared to A-type antiferromagnetic state for  $(\text{LaMnO}_3)_n(\text{SrMnO}_3)_{2n}$  with  $n=1$  and  $n=2$  on  $\text{SrTiO}_3$  substrate.

Since the supercell sizes and the numbers of each type of atoms are the same, we can simply compare the total energy of these two different superlattices. Since the A-type (C-type) magnetic structure is ferromagnetic (antiferromagnetic) within the  $ab$  plane and antiferromagnetic (ferromagnetic) along the  $c$  direction, we can approximately estimate an effective magnetic exchange ( $J_{\text{eff}}$ ) simply by comparing the total energy of the A-type and the

C-type antiferromagnetic states. It is clearly observed that the stabilization energy of the A-type antiferromagnetic state, i.e.,  $J_{\text{eff}}$ , is larger for  $n = 1$  than for  $n = 2$ . This implies that  $T_N$  for  $n = 1$  is higher than that for  $n = 2$ . These results are in excellent agreement with experimental observations by May *et al.* Since the epitaxial constraint of substrates is to fix the in-plane lattice constant  $a$  of the superlattices, the tetragonal distortion should inevitably occur, which in turn affects the relative occupation of Mn  $e_g$  electrons. We find that the  $\text{SrTiO}_3$  substrate induces tensile strain with  $a > c$ , in which the  $d_{x^2-y^2}$  orbital is lower in energy than the  $d_{3z^2-r^2}$  orbital. This can be seen in the projected charge density distribution, the integrated charge density from Fermi level down to  $-0.5$  eV indicating that  $e_g$  electrons preferably occupy the  $d_{x^2-y^2}$  orbital. Because of this orbital order induced inherently by the substrate strain, the A-type antiferromagnetic order is stabilized.

Remember that the magnetic interaction between Mn ions is determined by competition between the ferromagnetic double exchange via itinerant Mn  $e_g$  electrons and the antiferromagnetic superexchange between localized Mn  $t_{2g}$  electrons. When the  $d_{x^2-y^2}$  orbital is occupied rather than the  $d_{3z^2-r^2}$  orbital, the strong double exchange induces ferromagnetic order in the  $ab$  plane, while the weak itineracy of the  $d_{x^2-y^2}$  electrons along the  $c$  direction reduces substantially the double exchange and as a result, the superexchange between  $t_{2g}$  electrons stabilizes antiferromagnetic order along this direction. Finally, it is also interesting to note that the optimized lattice constant  $c$  for  $n = 1$  is shorter than that for  $n = 2$ , which is also qualitatively in good agreement with experimental observations.

#### B. $(\text{LaMnO}_3)_n(\text{SrMnO}_3)_{2n}$ on $\text{LaAlO}_3$

Now, let us study the electronic and the magnetic properties of  $(\text{LaMnO}_3)_n(\text{SrMnO}_3)_{2n}$  superlattices ( $n = 1, 2$ ) on (001)  $\text{LaAlO}_3$  substrate. In the alloy manganites  $\text{La}_{1-x}\text{Sr}_x\text{MnO}_3$ , TABLE II. The optimized lattice constant  $c$  (averaged value within the supercell and

in units of  $\text{Å}^\circ$ ) and  $c/a$  of  $(\text{LaMnO}_3)_n(\text{SrMnO}_3)_{2n}$  superlattices ( $n = 1, 2$ ) calculated using GGA. The magnetic structures are A-type and C-type antiferromagnetic for  $\text{SrTiO}_3$  and  $\text{LaAlO}_3$  substrates, respectively. It is known that  $c/a$  is a key parameter in determining the magnetic ground states. Here, we demonstrate that even in these superlattices, the magnetic structure

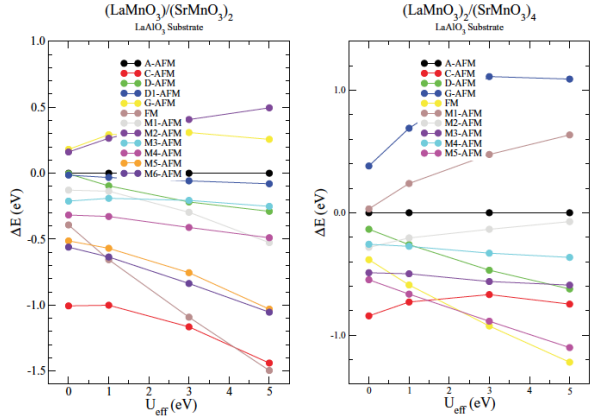


Fig.4  $U_{\text{eff}}$  dependence of the relative energies (calculated using GGA+U) for various magnetic structures compared to A-type antiferromagnetic state for  $(\text{LaMnO}_3)_n/(\text{SrMnO}_3)_{2n}$  with  $n=1$  and  $n=2$  on  $\text{LaAlO}_3$  substrate.

can be controlled by the substrate strain which varies  $c/a$ . Because the in-plane lattice constant of  $\text{LaAlO}_3$  is much smaller than that of  $\text{LaMnO}_3$  (bulk lattice parameter is  $3.935 \text{ Å}^\circ$ ), it is expected that the  $\text{LaAlO}_3$  substrate induces compressive strain. In fact, we find that the lattice constant  $c$  in the superlattices is larger than the in-plane lattice constant  $a$ . As a result of this tetragonal distortion, Mn  $e_g$  orbitals are split and the  $d_{3z^2-r^2}$  orbital is lower in energy than the  $d_{x^2-y^2}$  orbital, which thus induces  $d_{3z^2-r^2}$  orbital order. Because of this orbital order, the magnetic ground state is expected to be C-type antiferromagnetic. Considering 10–12 different candidates for possible magnetic structures as shown in Figs. 1 and 2, our GGA calculations find that the ground states for  $n = 1$  and  $2$  are both C-type antiferromagnetic metals [Figs. 1(b) and 2(b)]. It is also interesting to note that the lattice distortion along the  $c$  direction is less pronounced for the case

of  $\text{LaAlO}_3$  substrate as compared to the case of  $\text{SrTiO}_3$  substrate. Mn-O-Mn angles between the nearest layers along the  $c$  direction for the superlattices on  $\text{LaAlO}_3$  substrate are almost  $180^\circ$ , which certainly favors the ferromagnetic double exchange along this direction. We also find that the C-type magnetic structure is robust against electron correlations in Mn  $d$  orbitals up to  $U_{\text{eff}} = 4 \text{ eV}$  for  $n = 1$  and  $U_{\text{eff}} = 1.5 \text{ eV}$  for  $n = 2$  (See in Fig. 4). As in the case of  $\text{SrTiO}_3$  substrate, we can discuss the Néel temperature  $T_N$  for the C-type antiferromagnetic order by calculating the total energy. Simply by comparing the total energies of the C-type and the A-type antiferromagnetic states, the difference of which gives a rough estimate of an effective magnetic exchange  $J_{\text{eff}}$ , we find that the stabilization energy of the C-type antiferromagnetic state, i.e.,  $J_{\text{eff}}$ , is larger for  $n = 1$  than for  $n = 2$ . This implies that  $T_N$  for  $n = 1$  is higher than that for  $n = 2$ . Since  $(\text{LaMnO}_3)_n/(\text{SrMnO}_3)_{2n}$  superlattices ( $n = 1, 2$ ) on  $(001)$   $\text{LaAlO}_3$  substrate have not been studied experimentally, these results provide the theoretical prediction which should be tested experimentally in the future.

#### IV. SUMMARY

Using first-principles calculations based on the density functional theory, we have studied the effects of epitaxial strain on the magnetic ground states in  $(\text{LaMnO}_3)_n/(\text{SrMnO}_3)_{2n}$   $(001)$  superlattices with  $n = 1, 2$ . Our results clearly demonstrate that as in alloy manganites, even in superlattices, the epitaxial strain induced by substrates enforces tetragonal distortion, which in turn governs the ground-state magnetic structure via the inherent orbital ordering. We have found that for the tensile strain induced by  $\text{SrTiO}_3$   $(001)$  substrate, the ground state is A-type antiferromagnetic metal with  $d_{x^2-y^2}$  orbital order. The approximate estimation of an effective magnetic exchange suggests that the Néel temperature  $T_N$  of the A-type antiferromagnetic order is higher for  $n = 1$  than that for  $n = 2$ . These

## RICC Usage Report for Fiscal Year 2012

results are in excellent agreement with experimental observations. Furthermore, we have predicted that for the compressive strain induced by LaAlO<sub>3</sub> (001) substrate, the ground state is C-type antiferromagnetic metal with  $d_{3z^2-r^2}$  orbital order with higher Néel temperature  $T_N$  for  $n = 1$  than that for  $n = 2$ . These predictions should be confirmed experimentally in the future.

RICC Usage Report for Fiscal Year 2012

**Fiscal Year 2012 List of Publications Resulting from the Use of RICC**

**[Publication]**

Qinfang Zhang, Shuai Dong, Baolin Wang, and Seiji Yunoki, "Strain-engineered magnetic order in  $(\text{LaMnO}_3)_n/(\text{SrMnO}_3)_{2n}$  superlattices", Phys. Rev. B 86,094403 (2012).